

# Testing of Perpetual Pavement with Warm Asphalt Concrete Surface Mixes in the Ohio APLF

By

Shad M. Sargand  
Russ Professor of Civil Engineering  
Ohio University

William F. Edwards  
Research Engineer  
Ohio University

Juliàn Bendaña  
Engineer Research Specialist  
New York DOT

## Abstract

In September 2006, four lanes of asphalt concrete pavement were constructed in the Ohio Accelerated Pavement Loading Facility. One entire lane and one half of each of the three remaining lanes were constructed as a 16-inch (40.6 cm) thick perpetual pavement over 6 inches (15.2 cm) of 304 dense graded aggregate base (DGAB). The other half of the three lanes had reduced thicknesses of 13 (33.0), 14 (35.6), and 15 (38.1) inches (cm) of perpetual pavement over 9 (22.9), 8 (20.3), and 7 (17.8) inches (cm), respectively, of 304 DGAB to determine how dynamic responses and rutting on these sections compared to that measured on the 16-inch (40.6 cm) thick sections. The surface courses on these four lanes included conventional hot mixed asphalt concrete, and warm mix asphalt concrete containing Evotherm, Sasobit, and Aspha-Min. LVDTs, strain gauges, and pressure cells were installed in sections with the four pavement thicknesses to measure dynamic responses under rolling dual tires, and under an FWD load plate as surface deflections were measured at three nominal loads and three temperatures. Thermocouples were added to monitor temperature gradients in the pavement structures. Lateral profiles of the four lanes were recorded periodically to compare rutting of the four surface mixes and four pavement thicknesses under repeated applications of 9,000 lb. (40 kN) rolling dual tires at three temperatures.

The three warm asphalt concrete mixes had more early rutting under rolling wheel loads than the conventional mix, with Evotherm having the most rutting. Certain pavement responses were higher under 9,000 lb. (40 kN) dual tires rolling at 5 mph (8 kph) than under the FWD load plate at the same load.

## APLF Installation

Four lanes of asphalt concrete (AC) pavement, each eight-foot (2.44 m) wide and 45 feet (13.72 m) long, were placed adjacent to each other as a single pad in the Accelerated Pavement Loading Facility (APLF) in Lancaster Ohio. The entire length of Lane 4 and the northern half of Lanes 1, 2 and 3 had a build-up similar to a perpetual pavement constructed on Ohio U.S. 30 in 2005. The southern half of Lanes 1, 2 and 3 were constructed with thinner layers of 448 Intermediate AC to evaluate the effects of reduced AC thickness on dynamic response and

surface rutting under repeated rolling wheel loads. By increasing the thickness of the 304 dense-graded aggregate base (DGAB) by the same amount as the 448 Intermediate AC Layer was reduced, the combined AC/DGAB thickness and the elevations of the subgrade and pavement surfaces were the same in all pavement sections. All other material layers were the same thickness throughout the test pad. The surface courses on Lanes 1, 2 and 3 were warm asphalt mixes containing Evotherm, Sasobit, and Aspha-Min, additives which conserve energy and reduce emissions by lowering AC placement temperatures. Lane 4, which had a uniform design throughout and served as the control, had a conventional AC surface mix. The 22-inch (55.9 cm) thick AC/DGAB pad was placed on approximately 5 feet (1.52 m) of A6-A7 subgrade, and 12 inches (30.5 cm) of stone at the bottom of the concrete lined test pit. Figure 1 shows the build-up of Lane 1 with Ohio Department of Transportation (ODOT) material specifications, and Figure 2 is a plan view of the APLF test pad showing the layout of the eight test sections.

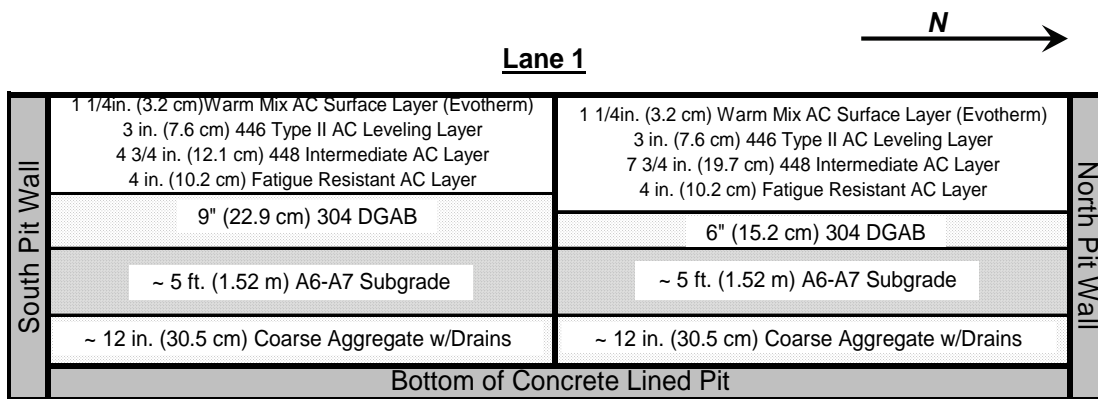


Figure 1 – Build-Up in Lane 1

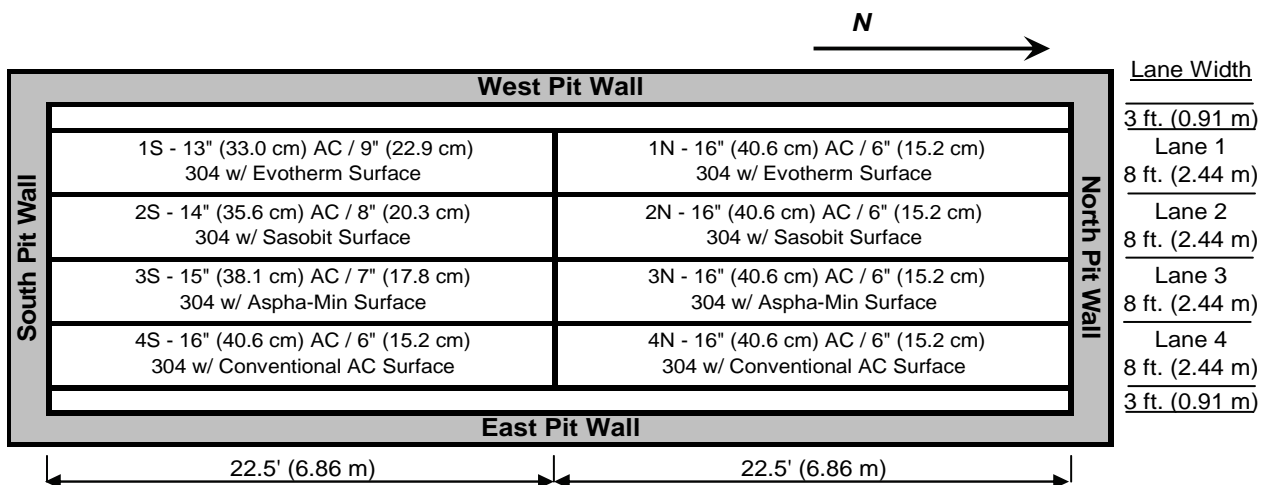


Figure 2 – Plan View of APLF Test Pad

Instrumentation installed in each of the southern pavement sections consisted of four Dynatest PAST II AC strain gauges, two Micro Sensors GHSD 750 LVDTs and one Geokon Earth Pressure Cell, all spaced 18 inches (45.7 cm) apart longitudinally along the lane centerlines to measure dynamic response of the four perpetual pavements of different thickness. Two strain gauges were mounted longitudinally and two transversely one inch (2.5 cm) above the bottom of the fatigue resistant AC layer to measure dynamic strain in the two directions. One LVDT was referenced to the top of the subgrade and one LVDT was referenced to about five feet (1.53 m) below the pavement surface to measure dynamic vertical deflections between the pavement surface and the reference elevations. The pressure cell measured vertical pressure at the top of the subgrade. Thermocouples were also placed one inch (2.5 cm) below the surface, at the center and one inch (2.5 cm) above the bottom of the AC layer to monitor temperature during the tests. Dynamic responses were recorded under the FWD load plate and the rolling dual tires.

### Test Plan

The overall test plan for the APLF installation consisted of measuring dynamic responses and surface rutting in the pavement sections at 40° F (4.4° C), 70° F (21.1° C) and 104°F (40.0° C), as follows:

- 1) Measure dynamic deflections with a Falling Weight Deflectometer (FWD) at nominal loads of 6, 000, 9,000 and 12,000 lbs.f. (26.7, 40.0 and 53.4 kN) in all eight sections.
- 2) Measure dynamic deflection, strain and pressure with sensors installed in the southern half of the test lanes during FWD testing and as 6, 000, 9,000 and 12,000 lbs.f. (26.7, 40.0 and 53.4 kN) loads were applied at 5 mph (8 kph) with rolling dual tires.
- 3) Periodically measure surface profiles in all eight sections as 10,000 rolling wheel loads were being applied at 9,000 lbs. (40.0 kN).

After air temperature in the facility had been maintained at 40° F (4.4° C) sufficiently long for temperature to stabilize throughout the test pad, dynamic deflections were measured with the FWD, and dynamic responses were measured with the embedded pavement sensors as loads were applied with the FWD and with rolling dual tires. Lateral surface profiles across the wheel paths were then measured at 0, 100, 300, 1,000, 3,000 and 10,000 passes of the rolling

dual tires. Similar data were then collected at nominal air temperatures of 70° F (21.1° C) and 104°F (40.0° C). For each of the three series of tests, temperature of the pavement surface was near the air temperature. At 70° F (21.1° C), temperature was about uniform with pavement depth. At 40° F (4.4° C) and 104°F (40.0° C), there was a slight gradient of increasing and decreasing temperatures, respectively, toward the bottom of the asphalt concrete.

### FWD Responses

FWD deflections were collected along the centerline of all pavement lanes at the three test temperatures. Three equally spaced tests were performed in the northern half of the lanes and the FWD load plate was placed over or near each of the seven response sensors installed in the southern half of the lanes. When the load plate was placed directly over holes housing the LVDTs, the geophone at the center of the plate could not be read. To avoid this problem, the FWD was offset laterally to allow all geophones to record valid data.

An individual FWD test consisted of three drops, one each at nominal loads of 6,000, 9,000 and 12,000 lbs.f. (26.7, 40.0 and 53.4 kN). Table I is a summary of average deflections measured during the second drop and normalized to a 9,000 lb.f. (40.0 kN) load. Deflections for Sections 1N, 2N, 3N, 4N and 4S are highlighted in Table I because these sections had the same structural build-up and would be expected to have similar responses for a given load and temperature. The consistent deflections shown for Df7 in Table I indicate uniform subgrade stiffness across the entire APLF pad.

FWD deflections showed a consistent trend of increasing with higher temperatures and a general, but not entirely consistent, trend toward lower deflections with thicker layers of AC. The differences in temperature were sufficiently large to cause the consistent trend in deflection, while the one inch (2.54 cm) changes in AC thickness resulted in deflection differences that fell within normal variations in FWD data. Reduced AC thickness was replaced with increased 304 DGAB thickness, which was less stiff than the AC but stiffer than subgrade.

The APLF pavements were assumed to be a three-layer system with Layer 1 being the AC, Layer 2 being 304 aggregate, and Layer 3 being A6-A7 subgrade. EVERCALC 5.0 was used to backcalculate moduli of the three material layers in all eight pavement sections from deflection profiles shown for these sections in Table I. These moduli are shown in Table II.

Table I  
Average Normalized FWD Responses by Section

Average Normalized FWD Deflection - mils / 9 kip (microns / 40 kN)										
Nominal Air Temp. °F (°C)	Section No.	Pvt. Thick. in. (cm)	Base Thick. In. (cm)	Geophone ID and Distance from Plate Center - in. (cm)						
				Df1	Df2	Df3	Df4	Df5	Df6	Df7
				0	8 (20.3)	12 (30.5)	18 (45.7)	24(61.0)	36 (91.4)	60 (152.4)
40 (4.4)	1N	16 (40.6)	6 (15.2)	1.84 (46.8)	1.51 (38.4)	1.43 (36.3)	1.33 (33.7)	1.20 (30.5)	1.01 (25.6)	0.65 (16.4)
	1S	13 (33.0)	9 (22.9)	2.58 (65.7)	2.12 (53.9)	1.99 (50.6)	1.81 (45.9)	1.58 (40.2)	1.25 (31.7)	0.71 (18.1)
	2N	16 (40.6)	6 (15.2)	1.98 (50.3)	1.58 (40.1)	1.50 (38.1)	1.40 (35.5)	1.27 (32.3)	1.07 (27.2)	0.69 (17.5)
	2S	14 (35.6)	8 (20.3)	2.67 (67.7)	2.22 (56.4)	2.08 (52.8)	1.85 (47.1)	1.63 (41.5)	1.28 (32.4)	0.74 (18.7)
	3N	16 (40.6)	6 (15.2)	2.01 (51.0)	1.65 (41.9)	1.57 (39.9)	1.48 (37.6)	1.33 (33.7)	1.11 (28.3)	0.72 (18.2)
	3S	15 (38.1)	7 (17.8)	2.37 (60.2)	1.97 (50.1)	1.85 (46.9)	1.70 (43.2)	1.50 (38.0)	1.21 (30.7)	0.70 (17.9)
	4N	16 (40.6)	6 (15.2)	2.17 (55.2)	1.77 (45.0)	1.66 (42.2)	1.53 (38.8)	1.38 (35.1)	1.11 (28.1)	0.65 (16.4)
	4S	16 (40.6)	6 (15.2)	2.43 (61.7)	1.93 (49.0)	1.79 (45.6)	1.67 (42.4)	1.48 (37.6)	1.23 (31.2)	0.73 (18.6)
70 (21.1)	1N	16 (40.6)	6 (15.2)	2.82 (71.6)	2.07 (52.5)	1.89 (47.9)	1.69 (42.8)	1.52 (38.7)	1.18 (30.0)	0.69 (17.5)
	1S	13 (33.0)	9 (22.9)	3.84 (97.5)	2.78 (70.7)	2.51 (63.8)	2.19 (55.7)	1.91 (48.4)	1.37 (34.9)	0.70 (17.9)
	2N	16 (40.6)	6 (15.2)	3.07 (78.0)	2.29 (58.2)	2.12 (53.8)	1.92 (48.7)	1.74 (44.1)	1.36 (34.7)	0.78 (19.9)
	2S	14 (35.6)	8 (20.3)	4.02 (102.2)	2.98 (75.7)	2.69 (68.3)	2.34 (59.5)	2.02 (51.3)	1.46 (37.1)	0.75 (19.0)
	3N	16 (40.6)	6 (15.2)	3.01 (76.5)	2.31 (58.7)	2.12 (54.0)	1.94 (49.2)	1.73 (43.9)	1.36 (34.7)	0.78 (19.9)
	3S	15 (38.1)	7 (17.8)	3.30 (83.9)	2.64 (67.1)	2.42 (61.3)	2.13 (54.1)	1.87 (47.5)	1.38 (35.0)	0.73 (18.6)
	4N	16 (40.6)	6 (15.2)	3.05 (77.6)	2.35 (59.6)	2.14 (54.5)	1.89 (48.1)	1.67 (42.5)	1.26 (32.0)	0.69 (17.5)
	4S	16 (40.6)	6 (15.2)	3.09 (78.4)	2.47 (62.8)	2.28 (57.8)	2.03 (51.5)	1.79 (45.5)	1.36 (34.7)	0.74 (18.7)
104 (40.0)	1N	16 (40.6)	6 (15.2)	4.98 (126.4)	2.67 (67.9)	2.36 (60.0)	2.03 (51.5)	1.76 (44.6)	1.28 (32.6)	0.67 (17.0)
	1S	13 (33.0)	9 (22.9)	5.88 (149.4)	3.44 (87.3)	2.93 (74.4)	2.43 (61.8)	2.03 (51.5)	1.39 (35.4)	0.68 (17.4)
	2N	16 (40.6)	6 (15.2)	4.49 (113.9)	3.05 (77.6)	2.74 (69.6)	2.38 (60.5)	2.06 (52.4)	1.52 (38.5)	0.79 (19.9)
	2S	14 (35.6)	8 (20.3)	6.01 (152.6)	3.64 (92.4)	3.12 (79.2)	2.56 (65.0)	2.12 (53.9)	1.44 (36.5)	0.70 (17.9)
	3N	16 (40.6)	6 (15.2)	4.71 (119.7)	2.97 (75.5)	2.64 (66.9)	2.27 (57.7)	1.97 (50.0)	1.44 (36.5)	0.75 (19.0)
	3S	15 (38.1)	7 (17.8)	4.93 (125.3)	3.21 (81.5)	2.78 (70.6)	2.34 (59.5)	1.96 (49.9)	1.37 (34.9)	0.69 (17.5)
	4N	16 (40.6)	6 (15.2)	4.64 (117.9)	2.92 (74.1)	2.57 (65.3)	2.17 (55.1)	1.83 (46.5)	1.29 (32.9)	0.65 (16.4)
	4S	16 (40.6)	6 (15.2)	5.00 (127.1)	2.87 (72.8)	2.65 (67.3)	2.26 (57.4)	1.92 (48.9)	1.38 (35.0)	0.70 (17.9)

Table II  
Backcalculated Moduli

Layer	Backcalculated Layer Moduli - ksi (GPa) - 3 Layers							
	South Sections				North Sections			
	1S	2S	3S	4S	1N	2N	3N	4N
<b>40° F (4.4° C)</b>								
E1	1842 (12.7)	1510 (10.4)	1783 (12.3)	1485 (10.2)	2187 (15.1)	1920 (13.2)	2091 (14.4)	1802 (12.4)
E2	16.3 (0.11)	12.9 (0.09)	6.4 (0.04)	9.4 (0.06)	16.2 (0.11)	28.1 (0.19)	11.6 (0.08)	5.0 (0.03)
E3	76.0 (0.52)	74.3 (0.51)	104.3 (0.72)	77.5 (0.53)	79.5 (0.55)	68.9 (0.48)	75.3 (0.52)	125.2 (0.86)
<b>70° F (21.1° C)</b>								
E1	808 (5.57)	708 (4.88)	956 (6.59)	1001 (6.90)	926 (6.38)	978 (6.74)	1029 (7.09)	908 (6.26)
E2	21.7 (0.15)	14.3 (0.10)	6.9 (0.05)	4.9 (0.03)	25.8 (0.18)	11.8 (0.08)	9.4 (0.06)	8.4 (0.06)
E3	66.8 (0.46)	66.3 (0.46)	89.4 (0.62)	100.5 (0.69)	68.0 (0.47)	66.6 (0.46)	70.5 (0.49)	84.1 (0.58)
<b>104° F (40.0° C)</b>								
E1	312 (2.15)	303 (2.09)	389 (2.68)	372 (2.56)	306 (2.11)	489 (3.37)	411 (2.83)	396 (2.73)
E2	37.2 (0.26)	23.9 (0.17)	19.5 (0.13)	21.0 (0.14)	62.0 (0.43)	12.3 (0.08)	20.5 (0.14)	16.6 (0.11)
E3	59.9 (0.41)	60.3 (0.42)	64.6 (0.45)	62.7 (0.43)	61.1 (0.42)	61.2 (0.42)	59.5 (0.41)	70.1 (0.48)

Sensor Responses under the FWD Load Plate

As the FWD was testing over the seven sensors embedded in each of the instrumented pavement sections, entire load pulses were recorded at the three loads and three temperatures. Table III is a summary of maximum sensor responses under the FWD load plate during the second drop and normalized to a 9,000 lb.f. (40.0 kN) load. LVDT data referenced to the top of the subgrade were not included in this table. These data show consistent trends of strain, deflection and vertical pressure increasing with temperature, but changes in response due to AC thickness were mixed. Again, this can be attributed to large differences in temperature and rather small differences in AC thickness. Longitudinal and transverse strains agreed quite well under the FWD load plate, which was expected because of the symmetrical loading.

Table III  
Measured Sensor Responses under FWD Load Plate

Measured Responses from Embedded Sensors under FWD Load Normalized to 9,000 Ibs.f. (40.0 kN)				
Nominal Air Temperature	1S (Evotherm)	2S (Sasobit)	3S (Asphamin)	4S (Control)
AC Thickness	13" (33.0 cm)	14" (35.6 cm)	15" (38.1 cm)	16" (40.6 cm)
Average Longitudinal Micro-Strain (Tensile)				
40° F (4.4° C)	12.5	20.2	16.1	10.1
70° F (21.1° C)	30.4	42.7	16.7	36.3
104° F (40.0° C)	55.6	70.4	52.2	51.6
Average Transverse Micro-Strain (Tensile)				
40° F (4.4° C)	17.3	22.7	18.0	15.1
70° F (21.1° C)	39.6	40.0	22.3	32.3
104° F (40.0° C)	51.3	49.8	51.3	47.7
Vertical Pressure on Subgrade - psi (kPa)				
40° F (4.4° C)	1.21 (8.35)	0.77 (5.32)	1.06 (7.34)	0.63 (4.36)
70° F (21.1° C)	3.06 (21.2)	2.52 (17.4)	2.27 (15.6)	1.42 (9.79)
104° F (40.0° C)	4.34 (29.9)	3.19 (22.0)	3.97 (27.4)	4.25 (29.3)
Deflection at Deep LVDT - mils (microns)				
40° F (4.4° C)	1.91 (48.5)	2.03 (51.5)	1.82 (46.2)	1.48 (37.6)
70° F (21.1° C)	2.04 (51.8)	4.42 (112)	2.20 (55.9)	2.34 (59.4)
104° F (40.0° C)	6.43 (163)	4.84 (123)	4.30 (109)	3.86 (98.0)

Deflection, strain and pressure responses corresponding to sensors installed in the pavement sections were then calculated with EVERSTRS 5.0 for a 9,000 lb.f. (40.0 kN) FWD load using moduli backcalculated with EVERCALC 5.0 for three-layer simulations of Sections 1S, 2S, 3S and 4S. A stiff layer was also added to account for the concrete bottom of the test pit and, while subgrade moduli were lower with the stiff layer, the overall agreement with actual response measurements was better with the three-layer simulation without the stiff layer. Calculated responses for the three-layer simulation are summarized in Table IV. Measured and calculated responses in Tables III and IV are in reasonably good agreement.

Table IV  
Calculated Sensor Responses under FWD Load Plate

Responses Calculated from FWD Deflections and Backcalculated Moduli				
Nominal Air Temperature	1S (Evotherm)	2S (Sasobit)	3S (Asphamin)	4S (Control)
AC Thickness	13" (33.0 cm)	14" (35.6 cm)	15" (38.1 cm)	16" (40.6 cm)
Average Longitudinal and Transverse Micro-Strain (Tensile)				
40° F (4.4° C)	18.2	19.4	15.6	15.8
70° F (21.1° C)	34.6	35.9	26.5	23.3
104° F (40.0° C)	63.3	63.6	48.5	44.3
Vertical Compressive Pressure on Subgrade - psi (kPa)				
40° F (4.4° C)	1.85 (12.8)	1.80 (12.4)	1.34 (9.24)	1.55 (10.7)
70° F (21.1° C)	2.89 (19.9)	2.65 (18.3)	1.86 (12.8)	1.59 (11.0)
104° F (40.0° C)	4.68 (32.3)	4.32 (29.8)	3.67 (25.3)	3.70 (25.5)
Deflection at Deep LVDT - mils (microns)				
40° F (4.4° C)	2.53 (64.3)	2.67 (67.8)	2.35 (59.7)	2.38 (60.5)
70° F (21.1° C)	3.68 (93.5)	3.92 (99.6)	3.29 (83.6)	3.08 (78.2)
104° F (40.0° C)	5.52 (140)	5.71 (145)	4.78 (121)	4.64 (118)

#### Sensor Responses under the Rolling Tires

On the same day the FWD tests were performed, output from the pavement sensors was recorded as a matrix of three loads and four lateral offsets were run unidirectionally with the rolling dual tires at 5 mph (8 kph). Loads were 6,000, 9,000 and 12,000 lbs. (26.7, 40.0 and 53.4 kN) and lateral offsets from the centerline were 0 (midpoint between the two tires), 2 inches (5.1 cm) (inside edge of dual tire), 7 inches (17.8 cm) (center of dual tire), and 12 inches (30.5 cm) (outside edge of dual tire). Table V shows average maximum longitudinal strain, average maximum transverse strain, maximum vertical deflection and maximum vertical pressure

measured at 0 offset under the 9,000 lb. (40.0 kN) rolling dual tire load at three temperatures. Normalization was not necessary for sensor responses under the rolling tires because earlier checks with platform scales indicated the applied loading was very accurate.

Table V  
Measured Sensor Responses under Rolling Wheel Load

Measured Responses from Embedded Sensors under Rolling Wheel Load = 9,000 lbs.f. (40.0 kN)				
Nominal Air Temperature	1S (Evotherm)	2S (Sasobit)	3S (Asphamin)	4S (Control)
AC Thickness	13" (33.0 cm)	14" (35.6 cm)	15" (38.1 cm)	16" (40.6 cm)
Average Longitudinal Micro-Strain (Tensile)				
40° F (4.4° C)	17.6	17.1	15.8	17.6
70° F (21.1° C)	37.2	40.4	29.6	33.3
104° F (40.0° C)	30.6	33.7	30.3	56.9
Average Transverse Micro-Strain (Tensile)				
40° F (4.4° C)	22.5	21.2	19.5	18.8
70° F (21.1° C)	54.9	58.3	38.1	33.6
104° F (40.0° C)	174.8	165.7	159.1	116.2
Vertical Pressure on Subgrade - psi (kPa)				
40° F (4.4° C)	1.50 (10.3)	0.74 (5.1)	1.24 (8.6)	0.86 (6.0)
70° F (21.1° C)	3.75 (25.9)	3.03 (20.9)	2.84 (19.6)	2.51 (17.3)
104° F (40.0° C)	7.59 (52.3)	6.66 (46.0)	6.64 (45.8)	6.22 (42.9)
Deflection at Deep LVDT - mils (microns)				
40° F (4.4° C)	2.24 (56.7)	1.97 (50.0)	1.80 (45.7)	1.93 (49.0)
70° F (21.1° C)	4.00 (102)	4.62 (117)	2.99 (75.9)	2.97 (75.4)
104° F (40.0° C)	7.47 (190)	11.1 (282)	9.95 (253)	7.23 (184)

While trends of increasing response with increasing temperature and decreasing AC thickness generally prevailed under the rolling tires, there were two major differences between responses under the FWD and the rolling tires. First, as temperature increased, transverse strain became much larger than longitudinal strain under the rolling tires and larger than transverse and longitudinal strains measured under the FWD load plate, which were about the same as longitudinal strain under the rolling tires. Second, the magnitudes of surface deflection and vertical pressure at the subgrade were much larger under the 5 mph (8.0 km/hr) rolling tires than under the FWD load plate at higher temperatures. Both observations confirm that rolling tire loads moving at creep speed induce certain higher responses on AC pavements than the FWD, which is designed to simulate vehicle loads traveling at normal highway speeds. Similar trends of speed dependent responses have been observed on other instrumented pavements in Ohio.

## Surface Rutting

Repeated wheel loads of 9,000 lbs. (40.0 kN) were applied in a bidirectional mode at 5 mph (8 km/hr.) with no lateral wander and the dual tires straddling the centerline in each lane. Bidirectional loading was selected to reduce test time, and small differences in rutting observed in earlier tests with bidirectional and unidirectional loading were considered negligible for this study. Transverse profiles were measured at two locations in each of the eight pavement sections prior to testing and averaged together after 100, 300, 1,000, 3,000 and 10,000 passes of the dual tires to determine rut depths. The profiles were measured from an arbitrary elevation and skewed across the lane so supporting feet on the 10-foot (3.05 m) long profiler would be located near the boundaries of the 8-foot (2.44 m) wide lanes to reduce any effects from AC deformation in adjacent lanes.

Fender washers were epoxied to the pavement surface for the profiler feet to sit on to minimize deviations in successive profile paths and reference elevations. The profiler consisted of a 2-inch (5.08 cm) diameter roller bearing mounted on an arm which pushed the bearing across the pavement surface and recorded elevations at 1/2 inch (1.3 cm) intervals along the profiles. To correct for any vertical displacement at the ends of the successive profiles, all profiles were aligned to the reference profile by: 1) moving vertically so the average of the first five points matched the average of the same five points on the reference profile, and 2) rotating entire profiles around the first point until the average of the last five points on each profile matched the average of the last five points on the reference profile. Figure 3 shows a typical profile history measured in Section 1S at 104° F (40.0° C). The heavy line is the initial reference profile recorded before any loads were applied at 104° F (40.0° C). This plot shows:

- 1) Zones of AC consolidation are bounded by inflection points on the profiles, the lateral position of which remained stable throughout the 10,000 loading cycles. The positions of these points varied slightly over the sixteen profiling locations on the test pad, probably due to slight variations in the layout of the fender washers, but were very close to the edges of the rolling tires at all locations.
- 2) Surface deformations across the wheelpath include elements of downward vertical consolidation under the tires, and horizontal shoving/upward vertical heaving outside the tires. For this study, deformation was limited to consolidation under the tires.

- 3) Initial consolidation in the wheelpaths was caused by earlier testing at 40° F (4.4° C) and 70° F (21.1° C), both of which resulted in minimal rutting and were considered to be seating runs for the 104° F (40.0° C) tests.
- 4) If rutting was measured with a straightedge, total deformation would be almost 0.5 inches (1.3 cm), which is often used as a criterion for grinding or overlaying actual pavements.
- 5) Undulations within the consolidated portion of the profiles under the tires were likely caused by the five treads in each tire, which remained in the same lateral position for all passes of the tires due to the lack of wander in the rolling wheel tests.

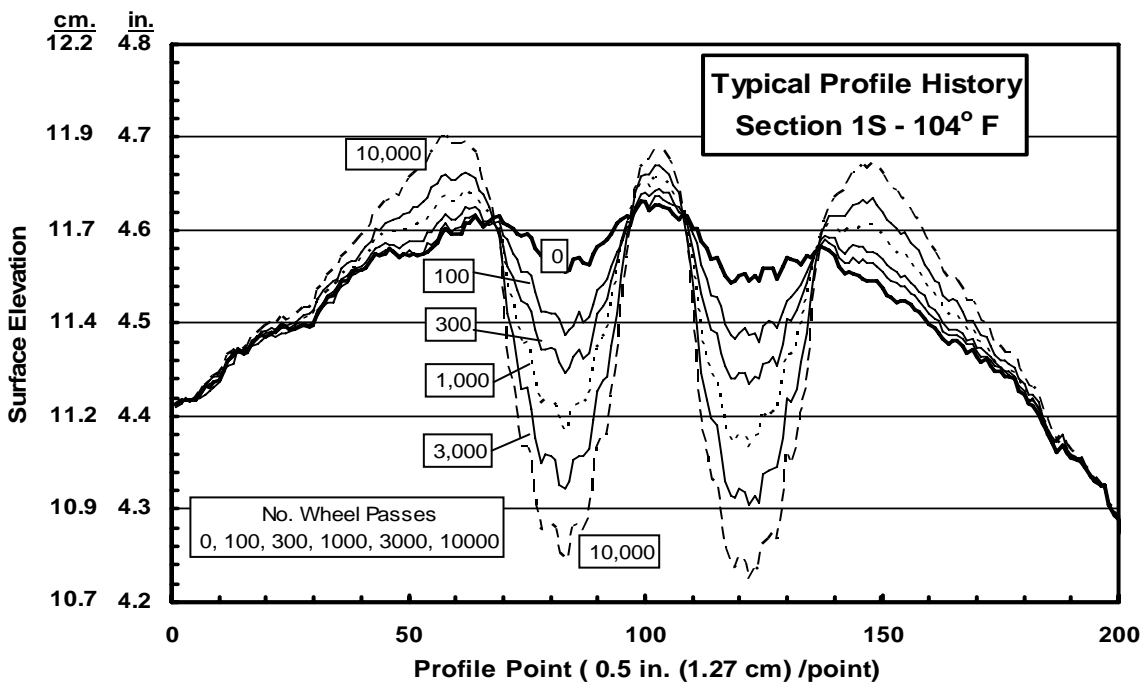


Figure 3 – Profile History in Section 1S

Average consolidation was calculated between the profile inflection points discussed above. Rutting at 40° F (4.4° C) was negligible over 10,000 rolling wheel passes, as profile differences were at or below profiler accuracy, which is 0.005 inches (0.13 mm) or less. At 70° F (21.1° C), average rut depths ranged from about 0.01-0.04 inches (0.25-1.02 mm) after 10,000 load cycles, but differences between early profiles and those near the tire edges were still at or below profiler accuracy. As shown in Figure 3, however, profile differences measured at 104° F (40.0° C) were well above profiler accuracy.

Figure 4 shows a linear plot of average consolidation on the 16-inch (40.6 cm) thick pavement sections with different surface mixes as 9,000 lb. (40.0 kN) rolling wheel loads were applied at 104°F (40.0° C). The three warm AC mixes in Lanes 1-3 had more consolidation in the initial 3,000 load cycles than the conventional mix in Lane 4, and then maintained a slightly lower rate of rutting than the conventional AC mix to 10,000 load cycles. Of the three warm AC mixes, Evotherm had more consolidation than Sasobit and Aspha-Min. The two redundant control sections with the conventional surface mix in Lane 4 agreed quite well and showed less consolidation than the warm AC mixes. While reasons for the higher early consolidation noted in the warm AC mixes are not known, it appears this effect dissipates rather quickly after the mixes are exposed to traffic loading, but the impact on rut depth is long term.

Figure 5 shows plots of consolidation in the three lanes where the warm AC surface mix was uniform throughout the lane, but thickness was different in the north and south sections of the lanes. Comparisons in this plot should be limited to a given lane where the only variable was thickness, or to the northern half of the lanes where the only variable was surface mix. In this plot, the thicker AC layers consistently showed more consolidation than their thinner counterparts, but the differences in consolidation were not proportional to thickness.

When plotted on a log-log plot in Figure 6, the consolidation data from all eight sections closely approximated straight lines with trendlines showing excellent correlation to equations of the form  $y = a x^b$  where  $y$  is the average depth of consolidation, Constant  $a$  is the  $y$  intercept calculated at one wheel pass,  $x$  is the number of wheel passes, and Constant  $b$  is the slope of the trendline. Table VI summarizes Constants  $a$  and  $b$ , and  $R^2$  calculated for the eight trendlines. In general, Constant  $a$  was larger and Constant  $b$  was smaller for the warm mix sections and the thicker AC sections. A comparison of values in Table VI and plots in Figures 4 and 5 show why Constants  $a$  and  $b$  are often considered as general indicators, but not accurate measures, of early and long-term consolidation, respectively. As an example of why Constant  $a$  is not a reliable measure of early consolidation, Section 3N with the Aspha-Min mix has the highest Constant  $a$  in Table VI, but Section 1N with the Evotherm mix clearly has the most early consolidation in Figure 4. This discrepancy was caused by the sensitivity of Constant  $a$  as trendlines are extrapolated back to one wheel pass. The timing of the first few profiles and the variability that occurs in these early measurements can have a significant impact on Constant  $a$ .

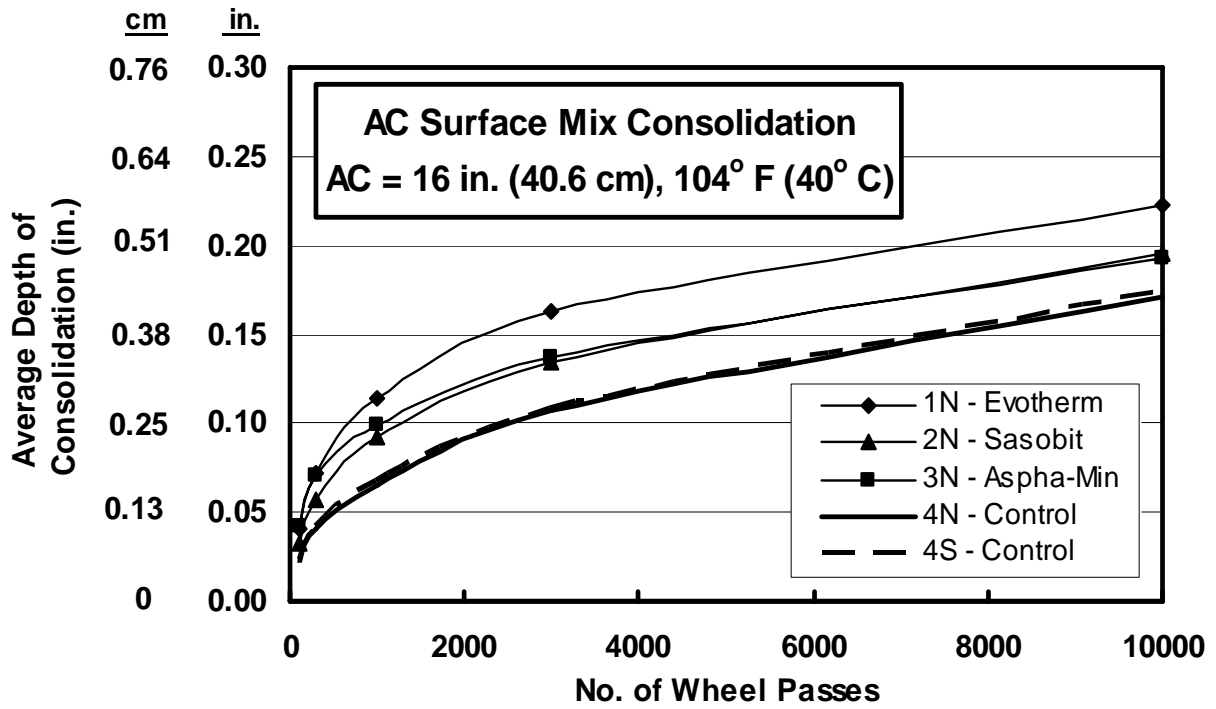


Figure 4 – Surface Mix Consolidation

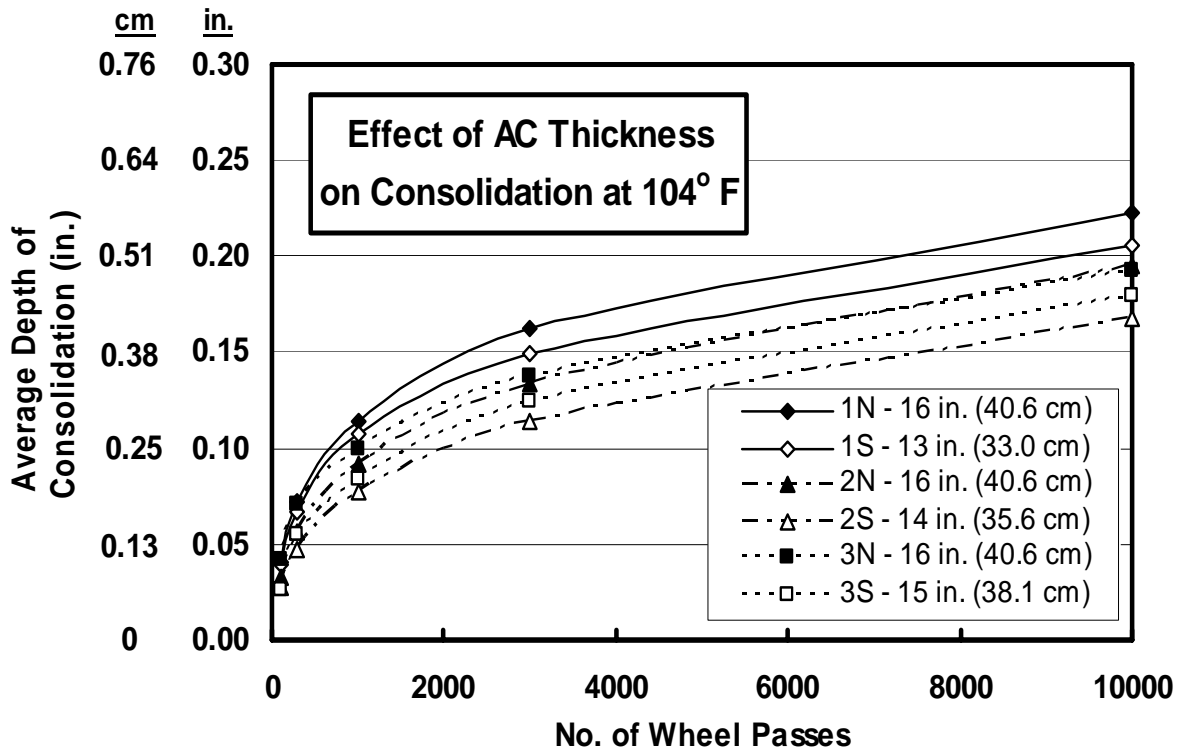


Figure 5 – Effect of AC Thickness on Consolidation

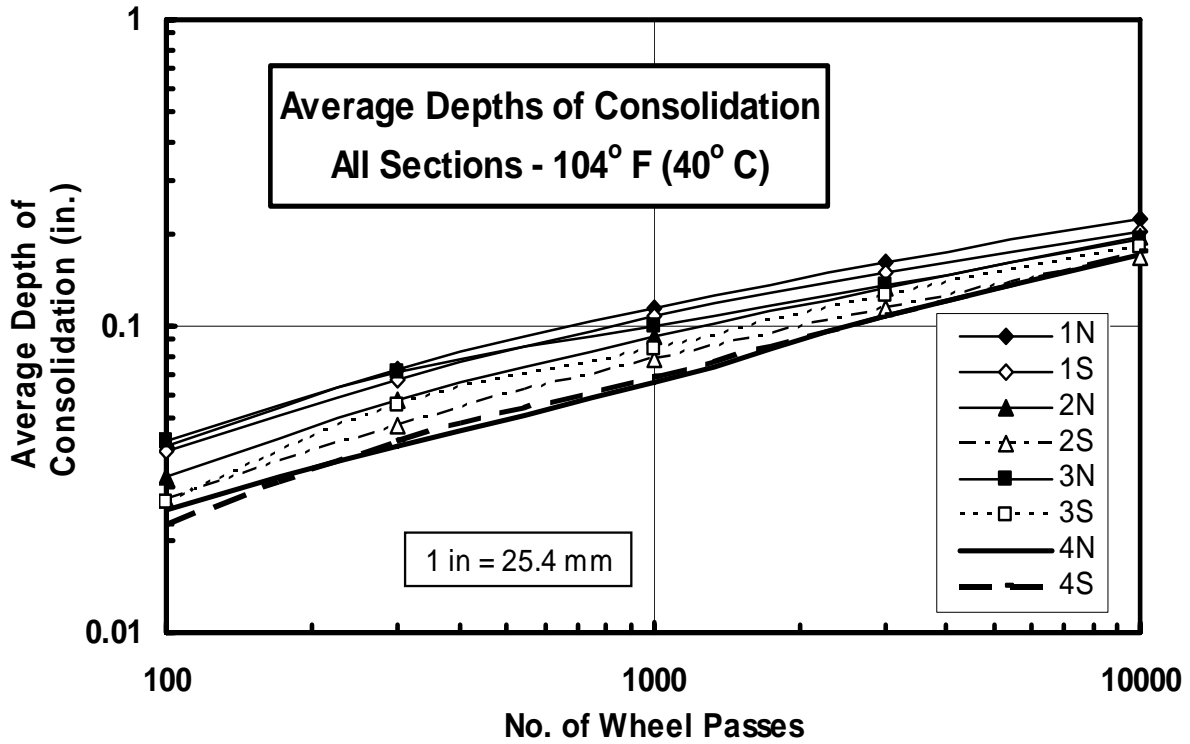


Figure 6 – Log-Log Plots of Average Consolidation

Table VI  
Constants and  $R^2$  for Consolidation Trendlines

Pavement Section	Trendline Parameters @ 104° F (40° C)			
	a (English)	a (Metric)	b	$R^2$
1N	0.0083	0.0211	0.3677	0.98
1S	0.0083	0.0211	0.3567	0.98
2N	0.0059	0.0150	0.3868	0.99
2S	0.0048	0.0122	0.3918	0.99
3N	0.0103	0.0262	0.3232	0.99
3S	0.0048	0.0122	0.4028	0.97
4N	0.0037	0.0094	0.4179	1.00
4S	0.0032	0.0081	0.4387	0.99

## Conclusions

1. FWD deflections consistently increased with higher temperatures and generally, but not always, decreased with thicker layers of AC. Temperature differences were sufficiently large to insure the consistent trend in deflection, but differences from the small changes in AC and 304 thickness were within normal variations observed in FWD data.
2. There were consistent trends of measured strain, deflection and pressure responses increasing with temperature, but not with AC thickness under the FWD load plate. This also can be attributed to the large differences in temperature and the rather small differences in AC and 304 thicknesses. Another observation was the general agreement of longitudinal and transverse stresses under the symmetrical FWD loading.
3. While trends of increasing response with increasing temperature and decreasing AC thickness generally prevailed under the rolling wheels, there were two major differences in responses measured with the FWD and the rolling wheels. First, transverse strains were much higher than longitudinal strains under the rolling wheels at higher temperatures, and higher than either strain under the FWD load plate. Second, the magnitudes of surface deflection and vertical pressure on the subgrade were much larger under the 5 mph (8.0 km/hr) rolling wheels than under the FWD load plate at higher temperatures. Both observations confirm that vehicles moving at creep speed induce higher responses than the FWD, which is designed to simulate vehicles traveling at normal highway speeds.
4. Deflection, strain and pressure responses corresponding to sensors installed in the pavement sections were calculated for Sections 1S, 2S, 3S and 4S using a three-layer simulation, a 9,000 lb.f. (40.0 kN) FWD load, and moduli backcalculated with EVERCALC 5.0. The measured and calculated responses showed good agreement.
5. Early consolidation of warm AC mixes under rolling tires was more than the conventional mix, after which the rate of consolidation was slightly less for the warm AC mixes than that for the conventional mix. Of the three warm AC mixes, Evotherm showed more consolidation than Aspha-Min and Sasobit, which were about the same.
6. In trendlines describing consolidation of the form  $y = ax^b$ , Constant  $a$  was larger and Constant  $b$  was smaller for the warm AC mixes and the thicker AC sections.

## References

1. Sargand, S., "Evaluation of Pavement Performance on DEL 23," Report FHWA/OH-2007-05, Ohio University, Athens, Ohio, 2007
2. Sargand, S., "Continued Monitoring of Instrumented Pavement in Ohio," FHWA/OH-2002/35, Ohio University, Athens, Ohio, 2002
3. Sargand, S., "Coordination of Load Response Instrumentation of SHRP Pavements," FHWA/OH-99/009, Ohio University, Athens, Ohio, 1999
4. Sargand, S., "Development of an Instrumentation Plan for the Ohio SHRP Test Pavement (DEL 23)," Ohio University, Athens, Ohio, 1994